

# Detection of Radio Emission by Cosmic Rays with the BEACON Prototype

A. Zeolla,<sup>a,\*</sup> J. Alvarez-Muñiz,<sup>b</sup> A. Cummings,<sup>a</sup> C. Deaconu,<sup>c</sup> V. Decoene,<sup>a</sup>

K. Hughes, R. Krebs, A. Ludwig, K. Mulrey, F. E. Oberla, S. Prohira, S.

W. Rodrigues de Carvalho, Jr., <sup>e</sup> A. Romero-Wolf, <sup>d,h</sup> H. Schoorlemmer, <sup>f,i</sup>

D. Southall, A. G. Vieregg, S. A. Wissel a, and E. Zas b

E-mail: azeolla@psu.edu

The Beamforming Elevated Array for COsmic Neutrinos (BEACON) is a novel detector concept consisting of many radio interferometers placed on mountaintops, searching for the radio emission of upgoing extensive air showers created when ultrahigh energy tau neutrinos skim the Earth. The BEACON prototype is located at the White Mountain Research Station in California at an elevation of 3.8 km and has been operating since 2018. It consists of a phased array of 4 custom, crossed-dipole antennas with a 30-80 MHz bandwidth. The prototype has demonstrated the ability to trigger on impulsive RF events in the presence of background noise, with at least one such event likely being a cosmic ray. The threshold of the prototype can be validated by a measurement of the cosmic ray flux, allowing us to better predict the sensitivity of a full-size BEACON to tau neutrinos. We discuss the goals of the BEACON concept, the status of the prototype, and an ongoing cosmic ray search which utilizes a convolutional neural network trained on simulated cosmic ray waveforms.

38th International Cosmic Ray Conference (ICRC2023) 26 July - 3 August, 2023 Nagoya, Japan



<sup>&</sup>lt;sup>a</sup>Dept. of Physics, Dept. of Astronomy and Astrophysics, Pennsylvania State University, University Park, PA 16802

<sup>&</sup>lt;sup>b</sup>Instituto Galego de Física de Altas Enerxías IGFAE, Universidade de Santiago de Compostela, 15782 Santiago de Compostela, Spain

<sup>&</sup>lt;sup>c</sup>Dept. of Physics, Enrico Fermi Institute, Kavli Institute for Cosmological Physics, University of Chicago, Chicago, IL 60637

<sup>&</sup>lt;sup>d</sup> Jet Propulsion Laboratory, Pasadena, CA 91109, USA

<sup>&</sup>lt;sup>e</sup>Department of Astrophysics/IMAPP, Radboud University, Nijmegen, The Netherlands

<sup>&</sup>lt;sup>f</sup> Nikhef, Science Park Amsterdam, Amsterdam, The Netherlands

<sup>&</sup>lt;sup>g</sup>Dept. of Physics and Astronomy, University of Kansas, Lawrence, KS 66045

<sup>&</sup>lt;sup>h</sup>Dept. of Astronomy, California Institute of Technology, Pasadena, CA 91109, USA

<sup>&</sup>lt;sup>i</sup>Department of High Energy Physic/IMAPP, Radboud University, Nijmegen, The Netherlands

<sup>&</sup>lt;sup>j</sup>Physics Dept., California Polytechnic State University, San Luis Obispo, CA 93407

<sup>\*</sup>Speaker

### 1. Introduction

Ultrahigh energy cosmic rays (UHECRs) interacting with photons are expected to result in a flux of high energy neutrinos. This can happen near the cosmic ray source (astrophysical neutrinos) [1] or while the cosmic rays propagate through cosmic photon backgrounds (cosmogenic neutrinos) [2]. Astrophysical neutrinos could be instrumental to identifying the sources of UHECRs as they are not deflected by magnetic fields, while cosmogenic neutrinos could provide information about acceleration mechanisms, source evolution, and UHECR composition [3].

Flavor oscillation results in an astrophysical neutrino flux with an even flavor ratio at Earth,  $v_e:v_\mu:v_\tau=1:1:1$  [4]. Ultrahigh energy (> 100 PeV) tau neutrinos which skim the Earth can produce a tau lepton which decays shortly after exiting the Earth, creating an upgoing extensive air shower (EAS) [5]. The charged particles present in the EAS are deflected by the Earth's magnetic field, resulting in coherent radio emission [6]. The Beamforming Elevated Array for COsmic Neutrinos (BEACON) is a detector concept designed to observe this radio emission. The concept consists of O(1000) autonomous phased antenna arrays placed on mountaintops. The high elevation site and long propagation length of radio waves gives each station a large detector volume. Each station is independent of the other, and as such they can be distributed globally providing nearly full sky coverage. The phased array trigger allows lower trigger thresholds by improving the signal-to-noise ratio and enabling the directional rejection of backgrounds.

A 1000-station BEACON, each array consisting of 10 short dipoles, is predicted to be sensitive to the cosmogenic neutrino flux [7]. A prototype of the BEACON concept is currently operating in the White Mountains of California. The prototype, in various iterations, has been running nearly continuously since 2018. The current prototype consists of 4 crossed-dipole antennas with a 30-80 MHz bandwidth. While unlikely to detect tau neutrinos with only a single station, the BEACON prototype is expected to detect O(1) cosmic rays a day [8]. Cosmic rays produce downgoing EAS, which like the upgoing EAS of tau leptons, emit radio. By measuring the cosmic ray flux we can confirm the energy threshold of the prototype and refine our full-scale sensitivity predictions. In section 2, we detail the current status of the prototype and discuss an impulsive event search performed last year. In section 3, we discuss an ongoing cosmic ray search which utilizes a convolutional neural network trained on simulated cosmic ray waveforms. Lastly, in section 4, we discuss future upgrades for the BEACON prototype.

#### 2. The BEACON Prototype

The BEACON prototype is located in the White Mountains of California, near White Mountain Research Center's Barcroft Field Station, at an altitude of 3.8 km. It consists of four dual-polarized antennas in a phased array, for a total of 8 channels. The antennas have a 30-80 MHz bandwidth and are elevated 13 ft above the ground so as to reduce ground interference. They are pointed East where the geomagnetic field most strongly deflects charged particles in extensive air showers. One antenna is pictured on the left in Fig. 1.

The dipole tines are fed into a 4:1 transformer which then leads to a 50  $\Omega$  low-noise amplifier. Coaxial cables then connect the antenna preamplifiers to the DAQ, pictured on the right in Fig. 1. In the DAQ, the signals are further amplified and passed through 30-80 MHz bandpass and FM



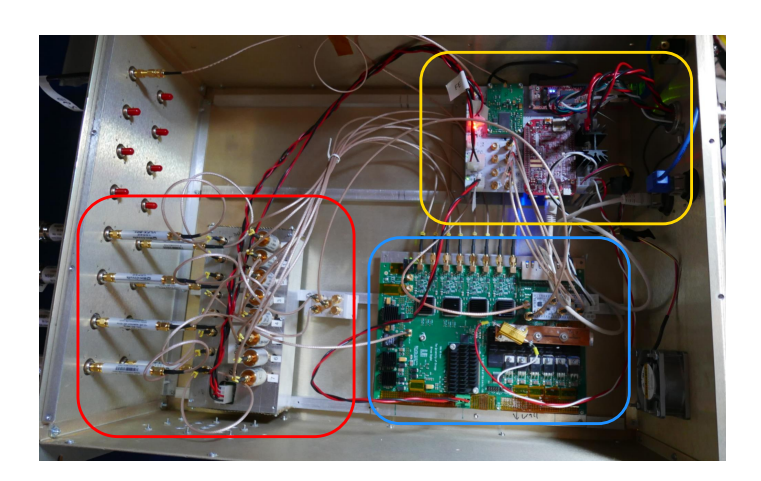


**Figure 1:** Left: One of the BEACON prototype crossed-dipole antennas. The antenna is elevated 13 ft off the ground and is pointed towards the valley to the East. Right: The BEACON prototype DAQ. The yellow box in the top right contains the single board computer, GPS clock, and power distribution. The red box in the bottom left contains the second stage amplifiers and filters. The blue box in the bottom right contains the digitizer and beamforming trigger board. Pictures sourced from [9].

notch filters. The signals are then digitized and passed to the beamforming trigger board. Radio signals emitted by a source reach each antenna in the array at a different time. The arrival time differences between all four antennas correspond to a specific source direction. The beamforming trigger uses a pre-calculated table of expected arrival time differences, called beams, to align the signals before summing them. Beamforming improves the signal-to-noise ratio by  $\sqrt{N_{antenna}}$ . The trigger rate is autonomously adjusted to be noise-riding. The trigger rate of each beam can be adjusted independently, so that backgrounds in a particular direction will not dominate the trigger.

A search was performed for impulsive, above-horizon events within ~112 days of RF-triggered data taken from the beginning of September to the end of December 2021 [9]. Cuts were performed based on reconstructed event direction, time delay clustering, impulsivity, and cosmic ray template correlation, among others. A cut removing below-horizon events removed 98% of events. In all, these cuts reduced ~100 million events to 5,440. These remaining events were inspected by hand and seemed to fall into three categories: mis-reconstructions of below-horizon events (4,081), airplanes (1,323), and unclassified events (36). Of these remaining unclassified events, at least one was likely a cosmic ray. The signal was highly impulsive and correlated well with a cosmic ray template, and the polarization was consistent with that of a cosmic ray from that direction. The waveforms, spectra, and reconstructed direction for this likely cosmic ray, event 5911-73399, are shown in Fig. 2.

#### 3. Ongoing Cosmic Ray Search

The previous search demonstrated the prototype's ability to trigger on impulsive above-horizon events, however it was designed to study all backgrounds to a neutrino search. We now seek to perform a truly automated cosmic ray search for the BEACON prototype. Since the BEACON prototype is expected to detect O(1) cosmic rays per day, and has been running continuously

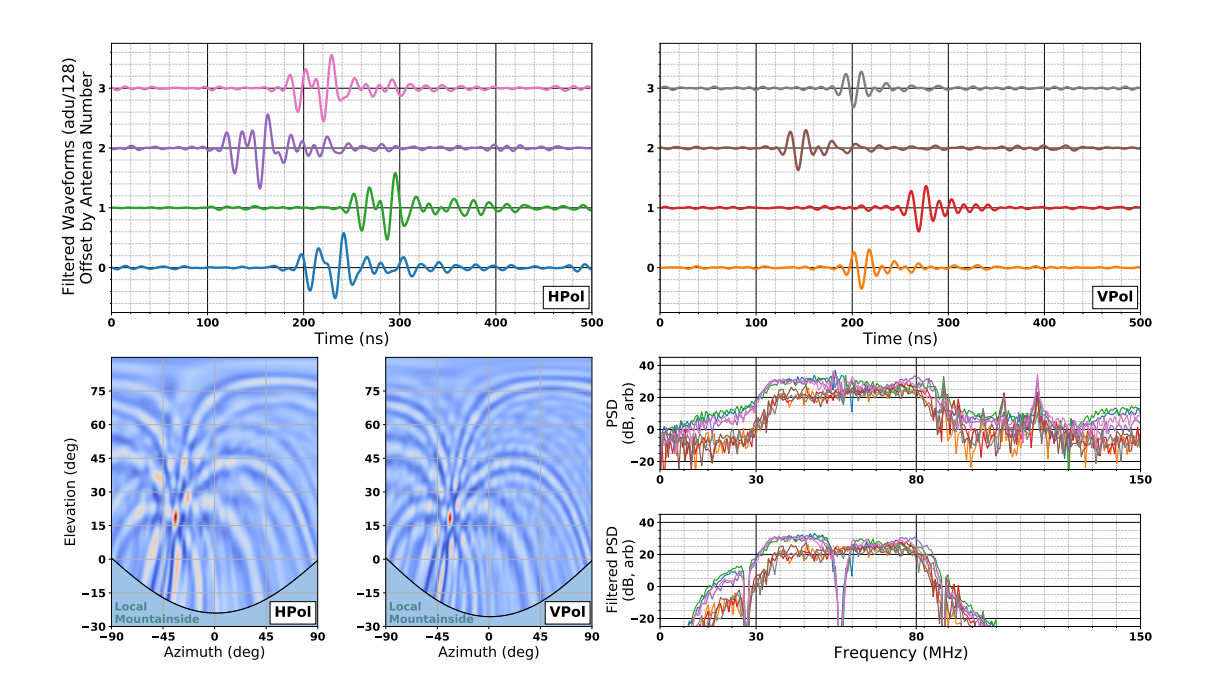


**Figure 2:** Event display for a likely cosmic ray event (Event 5911-73399). Top: Waveforms from each of the 8 channels, normalized and offset such that the y-axis indicates the antenna number for each waveform. Bottom Left: HPol and VPol correlation maps, individually normalized. Bottom Right: The Power Spectral Density (PSD) before and after filtering. Figure sourced from [9].

since 2018, there should be hundreds of detected cosmic rays among the hundreds of millions of RF-triggered events.

Cranberry, the cosmic ray simulation for BEACON [8], determines the electric fields received by each antenna for a given extensive air shower through the interpolation of a library of ZHaireS [10] simulations. The electric fields are converted to voltages using the XFdtd simulated impedance and gain of the antennas, and then finally convolved with the amplifier and filter signal-chain. In this way, Cranberry fully simulates the 8-channel waveforms of a detected cosmic ray. The goal is to use these simulated waveforms to identify real cosmic ray events.

Convolutional Neural Networks (CNNs) are highly effective at classifying 1-D time series, such as those output by the BEACON prototype [11]. CNNs are composed of an input layer, a series of hidden layers, and finally an output layer. Among the hidden layers are convolution layers which convolve their input with a matrix of tune-able filters before passing the resulting feature map onto the next layer. CNNs "learn" by iterating over data which has been grouped into classes. The CNN improves its classification accuracy by tuning the filters in its convolution layers such that the loss function is minimized. After a chosen number of iterations (epochs), or once accuracy ceases to improve, the CNN is done training. Passing an input to a trained CNN returns the probability of it belonging to each class. 1-D CNNs can be trained to classify single time series (univariate) or groups of time series (multivariate).

A CNN, based on the model used in [11], was constructed to classify cosmic rays. A diagram of the CNN model is shown in Fig. 3. The model was constructed using the Python interface Keras

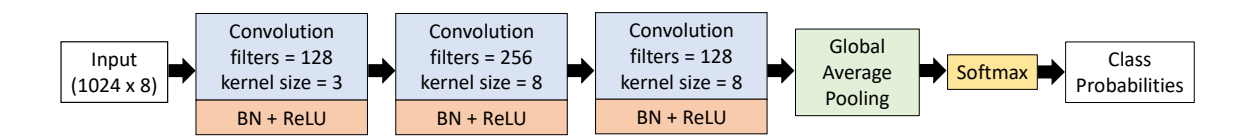


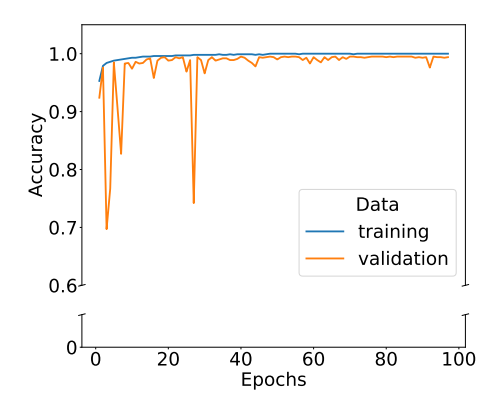
**Figure 3:** Structure of the Convolutional Neural Network constructed with Keras. The input (1024 samples, 8 channels) is passed through 3 convolutional layers. Each convolutional layer is followed by batch normalization and ReLU activation layers. The last 2 layers are global average pooling and softmax, after which the class probabilities are output.

and contains three 1-D convolution layers with filter sizes [128, 256, 128] and kernel sizes [3, 8, 8]. These hyperparameters were chosen using KerasTuner, which finds the optimal hyperparameters for a Keras model. Each convolution layer is followed by a batch normalization layer which normalizes the data. Following the batch normalization layers are ReLU activation layers which introduce non-linearity. Pooling layers are excluded to prevent overfitting. Instead of a fully-connected layer, a global average pooling layer is used because it is also less prone to overfitting. Global average pooling layers reduce feature maps to a single value, their global average. The last layer is a softmax layer which converts the vector of averages into a vector of probabilities based on their relative scale.

An event is composed of 8 time series with 1024 samples (2048 ns) each. When classifying an event, the CNN looks at all 8 channels together. This has an advantage over trying to classify events by single waveforms, as information like polarization angle would be lost. The CNN was trained on events grouped into three classes. In the first class were randomly sampled force-triggered events. These are events that are saved by the DAQ at a fixed rate of 2 Hz, regardless of the presence of a signal. As such, they are primarily noise. In the second class were RF-triggered events, randomly sampled over 100 runs. While some cosmic rays may be present in this dataset, they are predicted to make up less than 0.001% of RF-triggered events. This class therefore represents background signals which successfully triggered the array but are very likely not cosmic rays. The final class was composed of simulated cosmic ray signals from Cranberry added to randomly sampled force-triggered events.

To train the model, 25,000 events from each class were sampled. An additional 5,000 events from each class were used to validate the accuracy of the trained model. All 75,000 events were first sine-subtracted, a process that removes continuous-wave noise. The training accuracy and validation accuracy versus epoch are shown on the left in Fig. 4. Training concluded after 97 epochs, and the best model achieved a validation accuracy of 99.38%. On the right in Fig. 4 is a confusion matrix, which visualizes the model's classification accuracy. The classifier identified simulated cosmic rays within the validation data with 99.62% accuracy. It misidentified 0.36% and 0.02% of cosmic rays as force-triggers and RF-triggers respectively. Lastly, 0.22% of force-triggers and 0.16% of RF-triggers were misidentified as cosmic rays.

Given the expected rarity of cosmic rays relative to the total number of RF-triggered events, it is likely that additional cuts will be needed beyond classification by the CNN. Plotted in Fig. 5 are the reconstructed directions of 865,626 RF-triggered events during a 6 hour period on September 9, 2021. The vast majority of events are heavily clustered spatially, a property not expected of cosmic



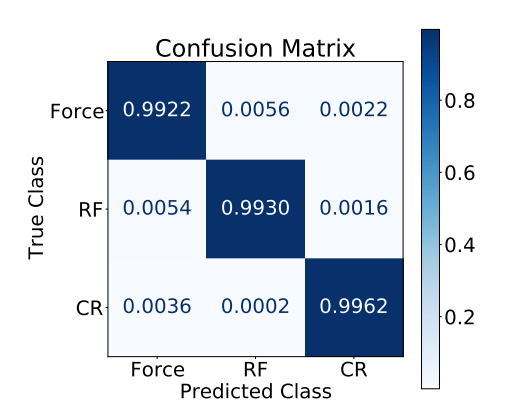


**Figure 4:** Left: CNN training accuracy and validation accuracy versus epoch. Training concluded after 97 epochs. Right: Confusion matrix for the validation dataset. Each entry in the matrix shows the fraction of events belonging to true class 'y' predicted to belong to class 'x' by the CNN.

rays. Additionally, cosmic rays should not be clustered in time. A temporospatial cut therefore seems like a logical additional cut. The same-source likelihood L between two events i and j is given by

$$-2\log\left(L_{ij}\right) = \left(\frac{\theta_i - \theta_j}{\sigma_\theta}\right)^2 + \left(\frac{\phi_i - \phi_j}{\sigma_\phi}\right)^2,\tag{1}$$

where  $\theta$  ( $\phi$ ) is the reconstructed zenith (azimuth) angle, and  $\sigma$  is the angular accuracy of the prototype. A temporospatial cut can be performed by finding the events j which occurred within some time window after event i, and then cutting those with a same-source likelihood larger than some chosen value (or equivalently, smaller than some  $-2 \log (L_{ij})$ ). Shown in the middle in Fig. 5 are the remaining events after a temporospatial cut was applied to the 865,626 RF-triggered events, using a time window of 60 seconds and same-source likelihood maximum of 0.368 ( $-2 \log (L_{ij}) = 2$  minimum), assuming  $\sigma_{\theta} = \sigma_{\phi} = 1^{\circ}$ . This cut eliminated 99.0% of events, suggesting that most background events are heavily clustered in time and space. On the right in Fig. 5 is the percent of events remaining as a function of time window size and  $-2 \log (L_{ij})$  minimum.

Additional cuts will be needed beyond the CNN classifier and temporospatial cut in order to sufficiently remove the large number of background events. Potentially useful cuts from the previous search include one which removes periodic noise (primarily due to arcing in the US power infrastructure), and another which checks for possible mis-reconstructions due to side lobes (detailed in [9]). The timestamp and location of passing events will also need to be cross-checked with aircraft tracking data to make sure no airplanes were present.

## 4. Future of the Prototype

Multiple upgrades to the prototype are being implemented in October, 2023. The DAQ is being upgraded to support up to 16 channels using a modular design. The new data acquisition system will include two FLOWER boards, originally designed for RNO-G [12] and modified for BEACON. Each FLOWER board hosts two commercially-available HMCAD1511 digitizer chips for 8 total channels with a configurable sampling rate. For the prototype, a 250 MSa/s sampling

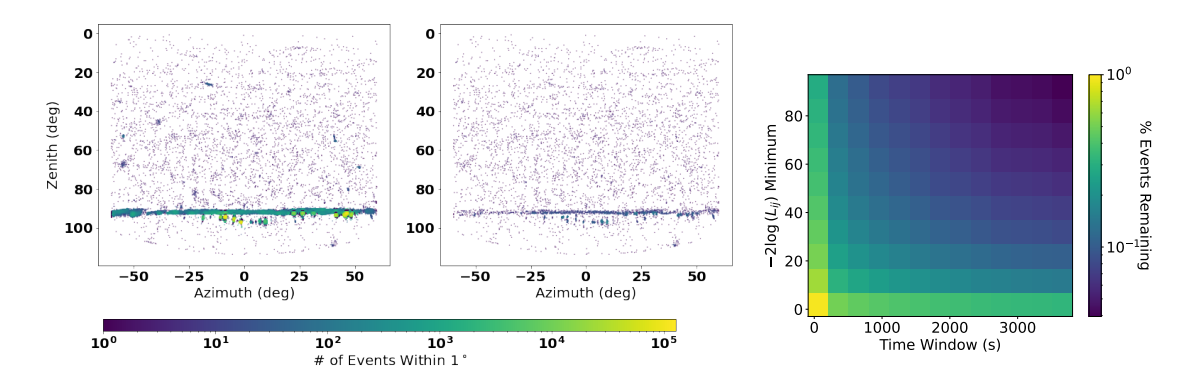


Figure 5: Left: Reconstructed source direction of 865,626 RF-triggered events during a 6 hour period on September 9, 2021. Middle: The remaining events after a temporospatial cut using a time window of 60 seconds and a same-source likelihood maximum of 0.368 was applied. 99.0% of events have been cut. Right: Percent of events remaining after a temporospatial cut, for different cut parameters. Event j occurring within some time window (x-axis) after event i is cut if  $-2 \log (L_{ij})$  is less than some minimum (y-axis).

rate will be used to capture the lowest 125 MHz of signal bandwidth, as well as an onboard FPGA for phased array triggering. The controller board can be further expanded in the future to include 24 channels if desired.

Four of these new channels will be used to deploy two additional cross-polarized antennas. While the new antennas will increase the sensitivity of the prototype, they are primarily being added to improve the interferometric reconstruction of events. Increasing the number of baselines will improve the pointing resolution and decrease the number of prominent side-lobes. All of the antenna feeds are planned to be upgraded to include a dual-band GPS patch antenna to calibrate the antenna phase centers and scan the local topography using GPS reflectometry techniques [13].

The four remaining channels will be used for a new scintillator array using the analog waveform readout and 2.4 m × 1 m scintillator panel originally developed for the IceTop experiment at the South Pole [14]. Scintillator arrays are not a planned feature of the full-scale instrument, but can help us study and improve the RF-detection capabilities of the current prototype. The four scintillator panels will be installed among the antenna array, parallel to the 20-30° slope of the mountainside, and will serve not only as a cosmic ray cross-check but also as a further study of inclined cosmic rays at high-altitudes. Background RF-triggered events are unlikely to also trigger the scintillator array. Events which are identified as cosmic rays during analysis of the RF-triggered data and coincident with a scintillator trigger are therefore very likely cosmic rays. This can be used to improve cosmic ray identification in RF-only data and to further tune the antenna array.

This work is supported by NSF Awards # 2033500, 1752922, 1607555, PHY-2012980, and DGE-1746045 as well as the Sloan Foundation, the RSCA, the Bill and Linda Frost Fund at the California Polytechnic State University, and NASA (support through JPL and Caltech as well as Award # 80NSSC18K0231). This work is also funded by Xunta de Galicia (CIGUS Network of Res. Centers & Consolidación ED431C-2021/22 and ED431F-2022/15), MCIN/AEI PID2019-105544GB-I00 - Spain, and European Union ERDF. We thank the NSF-funded White Mountain Research Station for their support. Computing resources were provided by the University of Chicago Research Computing Center. The Karlsruhe Institute of Technology (KIT) supported this project

with in-kind contributions of the scintillator array.

#### References

- [1] E. Waxman and J. Bahcall, *High energy neutrinos from astrophysical sources: An upper bound, Physical Review D* **59** (1998) .
- [2] V. Beresinsky and G. Zatsepin, *Cosmic rays at ultra high energies (neutrino?)*, *Physics Letters B* **28** (1969) 423.
- [3] M. Ackermann et al., Astrophysics Uniquely Enabled by Observations of High-Energy Cosmic Neutrinos, Bull. Am. Astron. Soc. **51** (2019) 185 [1903.04334].
- [4] J.F. Beacom, N.F. Bell, D. Hooper, S. Pakvasa and T.J. Weiler, *Measuring flavor ratios of high-energy astrophysical neutrinos*, *Phys. Rev. D* **68** (2003) 093005.
- [5] E. Zas, Neutrino detection with inclined air showers, New Journal of Physics 7 (2005) 130.
- [6] F.G. Schröder, Radio detection of cosmic-ray air showers and high-energy neutrinos, *Progress in Particle and Nuclear Physics* **93** (2017) 1–68.
- [7] S. Wissel et al., Prospects for high-elevation radio detection of >100 PeV tau neutrinos, JCAP 11 (2020) 065 [2004.12718].
- [8] A. Zeolla et al., The Beamforming Elevated Array for COsmic Neutrinos (BEACON): A Radio Detector for Earth-Skimming Tau Neutrinos, PoS ARENA2022 (2022) 023.
- [9] D. Southall et al., Design and Initial Performance of the Prototype for the BEACON Instrument for Detection of Ultrahigh Energy Particles, NIM-A 1048 (2023) 167889 [2206.09660].
- [10] J. Alvarez-Muñiz, W.R. Carvalho and E. Zas, Monte carlo simulations of radio pulses in atmospheric showers using ZHAireS, Astroparticle Physics 35 (2012) 325.
- [11] Z. Wang, W. Yan and T. Oates, *Time series classification from scratch with deep neural networks: A strong baseline*, 1611.06455.
- [12] RNO-G collaboration, *Design and Sensitivity of the Radio Neutrino Observatory in Greenland (RNO-G)*, *JINST* **16** (2021) P03025 [2010.12279].
- [13] K.M. Larson, M. MacFerrin and T. Nylen, *Brief communication: Update on the gps reflection technique for measuring snow accumulation in greenland, The Cryosphere* **14** (2020) 1985.
- [14] T. Huber, *IceScint: A Scintillation Detector Array for the IceCube IceTop Enhancement*, Ph.D. thesis, KIT, Karlsruhe, 2021. 10.5445/IR/1000131545.